Pressure-induced structural transitions of $LiNH_2$: A first-principle study

Yan Zhong [a], Huaiying Zhou [a,b], Chaohao Hu [b,c,*], Dianhui Wang [b], Guanghui Rao [b]

[a] School of Materials Science and Engineering, Central South University, Changsha 410083, PR China
[b] School of Materials Science and Engineering, Guilin University of Electronic Technology, Guilin 541004, PR China
[c] International Center for Materials Physics, Chinese Academy of Sciences, Shenyang 110016, PR China

ABSTRACT

The pressure-induced phase transformations in $LiNH_2$ have been studied by using *ab initio* total-energy calculations and evolutionary structure prediction simulations. Two stable high-pressure polymorphs of $LiNH_2$ are found: β-$LiNH_2$ (orthorhombic, $NaNH_2$-type, *Fddd*) and γ-$LiNH_2$ (orthorhombic, $P2_12_12$). The $\beta \rightarrow \gamma$ structural transition occurs at 10.7 GPa, which is in good agreement with experimental observation. Further analysis of the structural properties, charge density distribution, and calculated phonon density of states indicates that the possibility of the N–H···N hydrogen bond occurring in the high-pressure γ-$LiNH_2$ is extremely high. The existence of hydrogen bond weakens the N–H polar covalent bonds within NH_2 groups, which can facilitate the hydrogen desorption.

© 2012 Elsevier B.V. All rights reserved.

1. Introduction

To meet the requirements for efficient storage systems for the future vehicle applications powered by clean hydrogen energy, light metal complex hydrides have received considerable attention due to their high gravimetric hydrogen densities [1–5]. Among them, lithium amide ($LiNH_2$) has been extensively studied as a promising hydrogen storage material since Chen et al. [3] first reported that Li_3N can adsorb/desorb hydrogen in two-step reactions. At temperature below 300 °C, the reversible hydrogen capacity of $LiNH_2$ reaches to 6.5 wt.% under 0.04 and 20 bar [3]. However, its dehydrogenation temperature and hydrogenation pressure are still relatively high for practical applications. On the one hand, much effort has been devoted to further improving the thermodynamics and kinetics of the Li–N–H systems [6–9]. Price et al. [7] investigated the effects of different transition metal halides ($TiCl_3$, VCl_3, $ScCl_3$, and $NiCl_3$) on the sorption properties of the 1:1 molar ratio of $LiNH_2$ to MgH_2 and found that the hydrogen desorption temperature can be significantly reduced after adding these halides, particularly $TiCl_3$. Leng et al. [9] found that the additives of $MgCl_2$ with different amount can improve the H-desorption properties of Li–N–H system through different mechanisms. On the other hand, high-pressure polymorphism of light metal complex hydrides offers new insights because of the higher hydrogen density in them. First-principles investigation into the high-pressure structures of $LiBH_4$

demonstrated that the pressure-induced structural changes in BH_4 anions may decrease the activation energy for hydrogen desorption [10]. Chellappa et al. [11] found that during compressing and decompressing the ambient-pressure tetragonal $LiNH_2$ structure a reversible structural transition occurred in the pressure range 8–14 GPa. However, no detailed experimental structural data are yet available for its high-pressure polymorph. As stressed in our previous work [12,13], the structural information of a great number of light metal complex hydrides, especially of their high-pressure phases, is still missing, mainly due to the difficulty in determining the atomic position of light elements like hydrogen from the poor X-ray data.

Moreover, the question whether hydrogen bond appears in alkali metal amides like $LiNH_2$ and $NaNH_2$ is still open. Hydrogen bonding interactions in a solution or a compound generally cause the significant changes in their physical and chemical properties including frequency shifts of IR and Raman bands, dielectric constants, electrical conductivities, and altered freezing and boiling points [14]. The typical hydrogen-bonded systems like H_2O, NH_3, some organic molecules containing N–H groups, and related condensed phases have been extensively studied [15–17]. It is necessary to investigate the formation of hydrogen bond in inorganic amides due to the existence of special NH_2 groups in these structures. Although the previous IR and Raman studies reported that hydrogen bonds could not be observed in $LiNH_2$, $NaNH_2$, and even in their high-pressure phases [11,18,19], we explore the possibility of hydrogen bond formation in the high-pressure amide systems due to the ordering induced by pressure on the oriented amide ions. This is also motivated by our work [20] on $NaNH_2$ that has shown the presence of N–H···N hydrogen bond under high

* Corresponding author at: School of Materials Science and Engineering, Guilin University of Electronic Technology, Guilin 541004, PR China. Tel.: +86 773 2291 680; fax: +86 773 2290 129.

E-mail address: chaohao.hu@guet.edu.cn (C. Hu).

pressure. In this paper, our effort is mainly devoted to investigating the energetically favorable high-pressure phases of LiNH$_2$ in the different pressure ranges and their structural features in order to better understand its high-pressure behavior.

2. Computational details

To find the stable high-pressure structures of LiNH$_2$, an *ab initio* evolutionary algorithm (EA) as implemented in the USPEX (Universal Structure Predictor: Evolutionary Xtallography) code [21,22] was employed. Currently, many successful applications have indicated the EA simulations in USPEX are an effective way to search for the structures with the lowest free energy without requiring any experimental information [23,24]. In our present work, variable-cell structure simulations for LiNH$_2$ with one to four formula units (f.u.) at 0, 10, 20, and 40 GPa were performed to detect the lowest-enthalpy phases at different pressure ranges. Following the first generation of structure produced randomly, each subsequent generation was obtained from the lowest-enthalpy 60% structures of the preceding generation. The variation operators including heredity (65% structures), lattice mutation (25%), and atomic permutation (10%) were used for generating offspring. The underlying *ab initio* calculations were carried out by using a plane-wave method within the PBE exchange-correlation [25] as implemented in the Vienna Ab-initio Simulation Package (VASP) [26]. The electron-ion interaction was described by the all-electron projector augmented wave (PAW) scheme [27] and the electron configurations of $1s^2 2s^1$, $2s^2 2p^3$, and $1s^1$ were treated as valence for Li, N, and H, respectively. During structural relaxation an energy cutoff of 600 eV was used for the plane wave basis sets, and the k-point resolution smaller than $2\pi*0.03$ Å^{-1} in the reciprocal space was used for all structures in order to minimize the error from the k-point meshes. The atomic positions, lattice parameters, and cell volume were fully optimized with an iterative matrix diagonalization scheme until the total energy is converged to 0.1 meV/cell in the self-consistent loop and the force on each atom is less than 1 meV/Å.

Phonon calculations were carried out by the supercell method [28] as implemented in the FROPHO code [29], where the force constant matrices are obtained by displacing the atom inside the supercell and the phonon frequencies are directly derived from these matrices. In our work, the $2 \times 2 \times 1$, $2 \times 1 \times 2$, and $2 \times 2 \times 2$ supercells for α-, β-, and γ-LiNH$_2$ were constructed and the ±0.01 Å atomic displacements were used in all cases. For detailed comparisons with the experiments, the Raman spectra of high-pressure phases of LiNH$_2$ were calculated using the Quantum–Espresso (QE) package [30]. In our calculations, the norm-conserving pseudopotentials with local density approximation in Troullier–Martins type, a plane-wave cutoff energy of 80 Ry, and a $10 \times 10 \times 10$ Monkhorst-Pack mesh of k-points in the BZ integration were used.

3. Results and discussion

At 0 GPa, the ground-state tetragonal phase with space group I-4 (hereafter α-LiNH$_2$) and a metastable NaNH$_2$-type structure with space group $Fddd$ (hereafter β-LiNH$_2$) are identified from our EA search for the system with 16 atoms in unit cell, which is a correct result and confirms the robustness of EA for crystal structure prediction. In a higher pressure range from 10 to 40 GPa, an energetically favorable structure with space group $P2_12_12$ (hereafter γ-LiNH$_2$) is predicted from the EA simulations for systems with 8 and 16 atoms. The corresponding crystal structures of α-, β-, and γ-LiNH$_2$ are presented in Fig. 1. For the EA searches for systems 4 and 12 atoms in unit cell, two structures with the same space group $C2$ (for clarity, noted as $C2^*$ and $C2^{**}$, respectively) are detected.

By comparing the Gibbs free energies of any two phases, one can determine when the structural phase transition occurs. The Gibbs free energy $G = E + PV - TS$ becomes equal to the enthalpy $H = E + PV$, since all calculations in our work are performed at $T = 0$ K. Therefore, the high-pressure behavior of LiNH$_2$ can be well understood by comparing the static enthalpies of the above model structures as a function of pressure. As shown in Fig. 2, α-LiNH$_2$ is the most stable polymorph for pressures up to 4.6 GPa, at which it will transform into β-LiNH$_2$. However, it must be noted that the enthalpy difference between α- and β-LiNH$_2$ is tiny, only 1.2–3.2 meV/f.u. at pressures in the range of 0–4.6 GPa. Further increasing pressure to 10.7 GPa, γ-LiNH$_2$ becomes more stable than β-LiNH$_2$. A reversible structural transition for LiNH$_2$ detected from high-pressure Raman spectroscopy study [11] occurs in the pressure range from 8 to 14 GPa, which agrees well with our prediction. Crystal structure information of high-pressure phase of LiNH$_2$, however, is not available from the previous experiment. The identified γ-LiNH$_2$ with space group $P2_12_12$ is first reported in the present work. In addition, we must stress that it may be difficult to detect the structural transition from α- to β-LiNH$_2$ only depending on the present experimental techniques due to the tiny energy difference between α- and β-LiNH$_2$ as mentioned above. In fact, the small energy difference of only a few meV between two competing structures has also been thought to be beyond the accuracy of the present DFT-based calculations. The optimized structural parameters for α-(0 GPa), β-(4.6 GPa), and γ-LiNH$_2$ (10.7 GPa) are compiled in Table 1 and the available experimental parameters for α-LiNH$_2$ [31] are also listed for comparison. The calculated volume–pressure relation (see Fig. 3) shows that the changes in volume accompanying with the α → β and β → γ transitions are about 0.9% and 4.5%. Considering the structural relationship and lower energy barrier between α and β phases, the α → β transition can be easily implemented by slightly adjusting the atomic position of Li ions and orientation of NH$_2$ amide groups, which belongs to be a displacive transition. However, the transition from orientionally disordered β to ordered γ phase generally needs substantial structural modifications (i.e. breaking and reforming Li–N bonds), and should be reconstructive.

A structural similarity can be found in these competing crystal structures in which Li atoms are tetrahedrally coordinated by four NH$_2$ groups. Considering the pressure effect, however, a pronounced structural difference in the arrangement of the NH$_2$ groups and Li atoms can be found. As shown in Fig. 1a, the variation in the Li–N bond length in tetragonal α-LiNH$_2$ ranges from 2.064 to 2.220 Å and in the N–Li–N bond angles from 101.96° to 113.23°. The two N–H bond lengths in NH$_2$ group are slightly different from each other, about 1.027 and 1.028 Å. These results are in good agreement with the previous experimental data [31]. For β-LiNH$_2$ displayed in Fig. 1b, Li atoms and amide ions occupy Wyckoff positions of 16f and 16g. The N–H bond lengths in the NH$_2$ groups are exactly equal and about 1.026 Å at 4.6 GPa. The γ-LiNH$_2$ phase shown in Fig. 1c and d adopts a pronounced
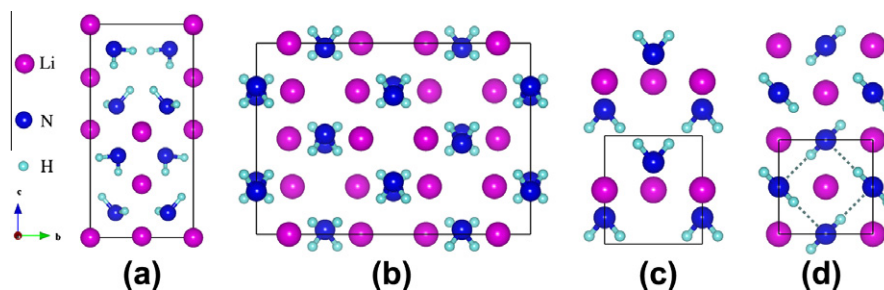

Fig. 1. Top view of stable crystal structures of LiNH$_2$ at different pressures: (a) α-LiNH$_2$ (I-4) at 0 GPa, (b) β-LiNH$_2$ ($Fddd$, NaNH$_2$-type) at 4.6 GPa, (c) and (d) γ-LiNH$_2$ ($P2_12_12$) at 10.7 GPa. The dashed lines depicted in (d) indicate hydrogen bond between [NH$_2$]$^-$ ions in γ-LiNH$_2$.